Published in final edited form as:

ACS Appl Mater Interfaces. 2016 January 13; 8(1): 802–808. doi:10.1021/acsami.5b10036.

Mutually-Reactive, Fluorogenic Hydrocyanine/Quinone Reporter Pairs for In-Solution Biosensing via Nanodroplet Association

Rajarshi Chattaraj[§,‡], **Praveena Mohan**[†,‡], **Clare M. Livingston**[†], **Jeremy D. Besmer**[†], **Kaushlendra Kumar**[†], and **Andrew P. Goodwin**[†,*]

[§]Department of Mechanical Engineering, University of Colorado Boulder. Boulder, CO 80309

[†]Department of Chemical and Biological Engineering. University of Colorado Boulder. Boulder, CO 80303

Abstract

Mutually-reactive, fluorogenic molecules are presented as a simple and novel technique for in-solution biosensing. The hypothesis behind this work was that aggregating droplets into close proximity would cause rapid mixing of their contents. To take advantage of this effect, a novel pair of fluorogenic redox molecules were designed to remain in lipid-stabilized oil droplets but mix once aggregated. First, the hydrophobic cyanine dye DiI was reduced with sodium borohydride to form a non-fluorescent analog (HDiI). Hydrophobic quinone derivatives were then screened as oxidizing agents, and it was found that p-fluoranil oxidized non-fluorescent HDiI back to fluorescent DiI. Next, HDiI and p-fluoranil were loaded into NEOBEE oil nanodroplets of average diameter 600 nm that were stabilized by a monolayer of DPPC, DSPE-PEG, and DSPE-PEG-biotin. Addition of streptavidin caused aggregation of droplets and the appearance of red fluorescent aggregates within 30 min. Next, Nanoparticle Tracking Analysis was used to record the fluorescence of the droplets and their aggregates. By integrating the fluorescence emission of the tracked droplets, streptavidin could be detected down to 100 fM. Finally, the droplets were reformulated to sense for Vascular Endothelial Growth Factor (VEGF), a biomarker for tumor metastasis. Using anti-VEGF aptamers attached to DSPE-PEG incorporated into the nanodroplet monolayer, VEGF could also be detected down to 100 fM.

Graphical abstract

[*]Corresponding Author: To whom correspondence should be addressed: andrew.goodwin@colorado.edu.

[‡]**Author Contributions**

The manuscript was written through contributions of all authors. All authors have given approval to the final version of the manuscript. These authors contributed equally.

Supporting Information. ^{1}H-NMR spectra of HDiI and reactivated product, fluorescence emission spectra, NTA droplet size distribution, NTA video frames, additional fluorescence/size scatterplots, and t-test results. This material is available free of charge via the Internet at http://pubs.acs.org.

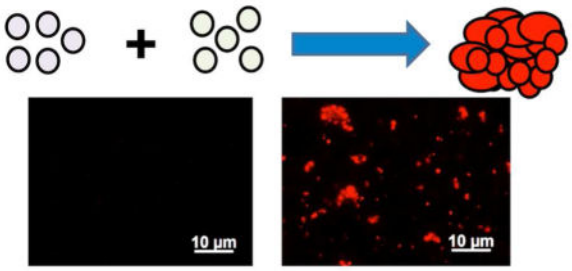

Keywords

Colloids; Self-Assembly; Sensors/Biosensors; Vascular Endothelial Growth Factor; Stimuli-Responsive Materials; Biomedical Applications

Introduction

Rapid, inexpensive detection of specific biomolecules is of tremendous importance for improving patient health, identifying infectious disease transmission patterns, and many other health-related goals. While ELISA is the gold standard of biomarker detection and quantification, its high cost and lengthy operation times inhibit wider utilization for routine assays. Detection of soluble analytes via sandwich assay has generally been achieved through the binding of an antibody bearing an additional moiety that can either serve as a label or amplify generation of detectable small molecules. In order to remove background signal, extensive washing steps are often required, increasing assay time and increasing the chances of operator error. A method that could provide a specific, detectable signal on a shorter time scale using inexpensive reagents would help to lower the barriers for more widespread assay development.

An alternative to a sandwich assay would be the generation of signal as a direct result of interaction with a specific biomarker in solution while minimizing background. Thus, signal must remain dark prior to mixing but become active once induced to do so during the detection phase. This method lends itself well to detection of enzymes that can naturally amplify activatable peptide-fluorophores.[1–2] Molecular beacons have also been designed to modulate their fluorescence intensity in response to nucleic acid or aptamer-bound analytes.[3–5] For more general analytes, aggregation is a highly customizable method of detection because it can be induced with antibodies. Examples include shifts in plasmon resonance for metal nanoparticles and antibody-tagged iron oxide nanoparticles that change their magnetic relaxivity upon aggregation.[6–9] However, in each of these cases, background signal can hinder specificity. For example, typical molecular beacon quenching or energy transfer ON-OFF ratios are usually 5–30 (85–97% quenching/transfer efficiency).[10–12] If instead the aggregation process were to cause the creation of signal rather than simply modulating it, a far greater specificity would be expected.

This paper presents an alternate strategy in which the aggregation of two oil droplets causes the mixing of two chemicals that react to produce an active fluorescent dye, thus creating fluorescence emission rather than shifting or modulating an existing signal. Previously, our

lab developed oil droplets that could be induced to fuse together and mix their contents via DNA-mediated interactions inspired by the SNARE complex.[13–14] In the course of performing these studies, we found that simple aggregation could also allow contents to pass across the lipid monolayer, leading to content mixing even without fusion. Thus, droplets bearing reactive payloads could potentially be used as in-solution biosensors via analyte-induced aggregation. In this work, this aggregation-based detection scheme was validated against streptavidin as a model analyte and against VEGF-165 as a biomarker for metastatic cancer.

Results and Discussion

Synthesis and Evaluation of Cyanine-based Switchable Fluorophore

To obtain efficient and rapid signal generation, redox reactions were chosen as a method of activation that could be made specific to droplet aggregation with some simple design rules. Redox reactions leading to unmasking of fluorescent dyes has been a highly successful approach for the sensing of Reactive Oxygen Species (ROS).[15–20] We theorized that the same effect might be obtained using oil-soluble oxidants. For the dye structure, we were directly inspired by hydride-reduced cyanine dyes developed by Murthy and coworkers[21–22] and Nagano and coworkers.[23] Here, 1,1′-dioctadecyl-3,3,3′3′-tetramethylindocarbocyanine perchlorate (DiI), a common membrane stain based on Cy5, was used instead because of its strong partitioning to an oil phase due to its two C_{18} chains. Reduced DiI (HDiI) was prepared by reacting with sodium borohydride in ethanol, followed by extraction and filtration through a silica plug (Figure 1A).[21–22] The resulting molecule was completely colorless and easily dispersible in different organic solvents (Figure 1B).

Next, the expected dye reactivation studies were tested in bulk. Initial studies showed that vegetable oils provided greater droplet stability than small molecule oils with less optical interference (data not shown). Thus, soybean oil and NEOBEE oil, a triglyceride extract of coconut oil, were examined as potential oil phases. For reagents, quinones were screened due to their oxidative reactivity and because many derivatives can be found as oil-soluble reagents. To screen reagents, equimolar amounts of HDiI and hydrophobic quinones were mixed in NEOBEE oil for 5 min, followed by recording of fluorescence emission spectra (λ_{exc} = 532 nm) (Figure 2A). Surprisingly, only some of the quinones reoxidized the HDiI effectively. Quinones with electron donating groups and additional ring structures such as 1,4-dihydroxyanthraquinone, 9,10-phenanthrenequinone, and 3,3′,5,5′-tetra-tert-butyldiphenoquinone yielded no appreciable change as compared to HDiI. All three benzoquinones with electron-withdrawing groups tested -- p-fluoranil (tetrafluoro-1,4-benzoquinone), p-chloranil, and DDQ -- yielded increase in signal, with p-fluoranil as the best, which also corresponded with the quinone possessing the highest oxidation potential.[24] Further optimization of p-fluoranil loading indicated that a 1:4 molar ratio of HDiI:p-fluoranil provided the greatest increase in fluorescence (51%); this formulation was utilized for all subsequent experiments (Figure 2B). To confirm that reaction proceeded as intended, ^{1}H-NMR spectra were obtained of commercial DiI alone, HDiI alone, and 1:4 HDiI:p-fluoranil. The spectra show that mixing HDiI and p-fluoranil results in a clear reappearance of the original peaks found in the commercial DiI sample, albeit with some

broadening (Figure S1). The formation of DiI was confirmed by both ^{1}H-NMR spectra and ESI-MS (see Supporting Information). The incomplete recovery of fluorescence is thus most likely due to side bleaching reactions caused by the presence of strong oxidizers. In addition, mixtures of HDiI and p-fluoranil did not fluoresce as strongly in soybean oil, possibly due to side reaction between the unsaturated tails in the oil and the p-fluoranil (Figure S2).

Nanodroplet Formulation and Aggregation

For proof-of-concept sensing experiments, nanodroplets containing either HDiI or p-fluoranil in NEOBEE oil were stabilized by a monolayer of lipid and polymer-lipids containing biotin (Figure 3A). Addition of streptavidin to these biotin-containing droplets would cause the formation of aggregates and activation of fluorescence (Figure 3B). To make the droplets, a lipid film containing DPPC, DSPE-PEG2000, and DSPE-PEG2000-Biotin was first hydrated in Tris Buffered Saline (TBS) to form liposomes. To this, a 4 v/v% solution of NEOBEE oil containing either HDiI or p-fluoranil was added, and the mixture was probe sonicated to obtain an emulsion suspension, which was then centrifuged through a 0.45 μm filter to reduce size polydispersity. Measurements by Nanoparticle Tracking Analysis (NTA) determined both the concentration and the size (mean diameter 575.5 ± 203.5 nm) of the nanodroplets (Figure S3).[25] To show that aggregation led to fluorescence activation, equal concentrations of droplets were mixed with varying concentrations of streptavidin and the resultant aggregates were imaged by fluorescence microscopy. For mixed droplets without streptavidin, a small amount of signal was observed by microscopy (Figure 3C). However, addition of 25 nM (Figure 3D) and 1 μM (Figure 3E) streptavidin caused the formation of aggregates that were clearly visible by fluorescence microscopy. Since increased fluorescence should primarily arise from mixing of reagents, one question is the mechanism by which the reagents encounter one another. While small amounts of droplet fusion are certainly possible, the appearance of some signal in the absence of streptavidin – and hence, aggregation – indicates that the internal phase may diffuse through one monolayer and into another droplet. Thus, while the probability of a molecule diffusing out of one droplet and into another is much higher when the droplets are aggregated, a small amount of reagent, probably p-fluoranil rather than HDiI, is likely able to diffuse through the aqueous media as well. Nevertheless, the fluorescent signal is clearly greater for aggregated droplets than unaggregated as a direct result of streptavidin addition.

Sensing of Streptavidin via Droplet Association

Studies were performed to illustrate the ability of this system to perform biosensing. One complication was that the nanodroplets scatter light, which interfered with bulk fluorescence measurements. However, a method that could specifically select fluorescent droplets would be able to overcome this limitation. The NTA instrument records video of particle suspensions, records Brownian motion of the particles, and calculates particle size via the Stokes-Einstein equation (Figure S4). By irradiating the particles at 532 nm and applying a red fluorescence emission filter, the NTA could specifically select for droplets that contained red fluorescence only, thereby reducing background from non-fluorescent droplets. No additional thresholding was necessary.

In a typical experiment, suspensions of HDiI droplets and p-fluoranil droplets were combined as above with a series of streptavidin concentrations from 100 fM-25 nM at 37°C for 30 min. Droplets were then excited at 532 nm while monitoring their motion and fluorescence emission for 60 s, thus both recording droplet diffusivity and fluorescence intensity simultaneously. The emission of each fluorescent droplet was integrated over the 60 s of video acquisition (example stills in Figure S4). The resultant scatter-plots show that droplet samples containing streptavidin have larger sizes and fluorescence intensities than those without (Figure 4A–B, Figure S5). To quantify the relative responses between the samples, the integration of intensities of all fluorescent droplets and aggregates detected by the NTA was plotted as a function of streptavidin concentration (Figure 4C). This method showed a clear differentiation between the integrated signals between the control sample and an analyte concentration as low as 100 fM. At this concentration and the others tested the p-value for a one-tailed t-test was < 0.05. Interestingly, the dynamic range of this study also has a theoretical upper limit as defined by the size of the resultant aggregates. As shown in our previous work with fluorocarbon droplets, above a certain streptavidin concentration droplets tend to form higher order aggregates rather than smaller clusters, but their slow diffusion restricts the maximum detectable size to 2 μm.[26]

As discussed above, the background signal in the absence of streptavidin was probably caused due to some amount of diffusion of the p-fluoranil first into the aqueous solution and then into a HDiI-loaded droplet. To measure the effect of this process on background signal generation, HDiI and p-fluoranil loaded droplets were incubated at 37°C and the resulting response was measured by NTA. As expected, simply mixing the droplets caused some increase in integrated signal over time, but the signal reached only to a level corresponding to close to 1 pM streptavidin even after 2 hrs of agitation (Figure 5A). Another potential complication was sensing capability in more complex media. HDiI and p-fluoranil loaded droplets were incubated with and without 1 nM streptavidin in either 50% Fetal Bovine Serum (FBS) and in 50% Sodium Citrate-stabilized bovine plasma. Based on the response, streptavidin-mediated aggregation clearly occurred in both FBS and plasma (Figure 5B). Little change was observed for the samples without streptavidin, supporting the specificity of response and the stability of the HDiI to complex media. For samples with streptavidin, signal was overall less intense and more variable for serum and plasma than for buffer, which indicates that specificity of sensing is governed by the analyte capture agents (e.g. aptamers and antibodies) rather than the droplets themselves. For comparison, previous research in our labs showed that fluorocarbon droplets with similar lipid compositions showed little nonspecific activation by off-target analytes.[26] Most likely, the serum proteins bind nonspecifically to the lipid shell, reducing diffusion of p-fluoranil from the droplets. Another possibility is the consumption of p-fluoranil via side reaction with a serum protein, which has been observed previously.[27–28] Nevertheless, the presence of complex media only reduces overall signal by about 25%.

Aptamer-VEGF binding and Droplet Aggregation

To validate the nanodroplet sensors with a more biomedically relevant analyte, we next reformulated the droplets to sense for Vascular Endothelial Growth Factor A (VEGF). VEGF has been sensed previously using ELISA, microfluidic chips, and microarray

techniques.[29–32] The crystal structure has shown that VEGF exists as an antiparallel homodimer, and thus containing two binding sites that will allow association of droplets on other side of the dimer.[33] While VEGF antibodies are commercially available, we sought to decrease the distance between bound droplets by using VEGF aptamers, thereby improving content transfer.[34, 35] The reported anti-VEGF aptamer was utilized here with the following modifications: (1) both 5′-CCC and GGG-3′ were incorporated at the termini to stabilize the folded conformation for improved association,[34, 35] (2) an additional 5′-TTTT spacer to provide flexibility for binding to VEGF dimer, and (3) the 5′ end was thiolated for conjugation (see Experimental for full sequence). The thiolated anti-VEGF aptamer was then reacted with DSPE-PEG2000-Maleimide in the presence of Tris(2-carboxyethyl)phosphine hydrochloride) (TCEP) to allow incorporation of the aptamer into the droplet monolayer as a conjugate (DSPE-PEG2000-Mal-Apt).

In-solution detection of VEGF dimer was performed analogously to the streptavidin sensing studies. Nanodroplets loaded with HDiI and p-fluoranil were formulated using a lipid-PEG stock solution, but with the DSPE-PEG2000-Mal-Apt in place of the DSPE-PEG2000-Biotin. Fluorescence microscopy images of these droplets without and with 100 nM VEGF are shown in Figure 6A and Figure 6B respectively. As with streptavidin, aggregation of droplets led to mixing of HDiI and p-fluoranil diffusion through the droplet monolayers, generating a fluorescence signal. In the absence of VEGF, apparent fluorescence was low by microscopy (Figure 6A). Next, HDiI and p-fluoranil droplets were incubated with varying concentrations of VEGF in TBS to determine a dose response trend. NTA was once again performed on the droplets under a 532 nm excitation laser through a fluorescence filter. A similar trend of integrated signal vs. analyte concentration was observed as for streptavidin (Figure 6C). The integrated signal leveled at higher concentrations, probably due to formation of larger aggregates and the limitation of NTA to detect aggregates greater than 2 μm in size as described above. Without VEGF there was more background signal than for streptavidin, possibly due to increased non-specific aggregation caused by non-complementary association of aptamer strands. However, these results show that VEGF-165 homodimers can be detected by this technique down to 100 fM (~ 4 pg/mL), with the greatest dynamic range between 100 fM to 10 pM (~400 pg/mL). These levels correspond well with an ability to differentiate serum VEGF levels from normal baseline (150 pg/mL) to elevated levels associated with metastatic breast cancer (320 pg/mL).[32] For comparison, commercial ELISA assays such as the Human VEGF Immunoassay (R&D Systems) are able to obtain greater difference in signal between these levels and with a linear signal-concentration dependence. However, the reported fluorogenic system is able to obtain results within 30 min as compared to >4 h for solid-phase ELISA assays such as these (R&D Systems). Interestingly, the detection limit for VEGF-165 was similar to that of streptavidin, even though the dissociation constants of VEGF-165/aptamer and streptavidin/biotin are quite different (~50 nM[34] and 10 fM, respectively). We attribute this finding to diffusion of p-fluoranil from the droplets, which generates background signal that reduces sensitivity for the streptavidin/biotin assay. Future studies will thus focus on designing other reactive pairs that will partition more effectively into the droplets with the aim of reducing background and improving limit of detection.

Conclusion

In summary, a novel fluorogenic system was developed as an in-solution biosensor. Oil-soluble DiI, a hydrophobic cyanine derivative, was reduced into a non-fluorescent molecule. A series of quinones were found to be able to partially restore the reduced DiI to fluorescence. Biosensing was performed by placing HDiI and p-fluoranil in separate biotinylated droplets, followed by addition of varying concentrations of streptavidin. Droplet aggregates were found to become fluorescent as observed by microscopy. By counting the total fluorescence of the droplets by Nanoparticle Tracking Analysis, streptavidin could be sensed down to 100 fM. The background oxidation of the HDiI was found to be slow enough to allow detection in 30 min, and the signal was found to activation with about 25% less activity in serum and plasma. Finally, this same system was able to detect Vascular Endothelial Growth Factor A down to 100 fM using aptamer-analyte interactions. In future studies, the work described here will be expanded to sense for more complex analytes via antibody interactions.

EXPERIMENTAL SECTION

General information

Fluorimetry studies were performed on a Photon Technology International fluorimeter with lamp power supply model LPS-220B, motor driver model MD-5020, and shutter control model SC-500. ^{1}H-NMR studies were performed on a Bruker AV-III 400 MHz NMR spectrometer with ICON NMR in automation, while ^{13}C NMR studies were run at 100 MHz. $CDCl_3$ was used as solvent, chemical shifts are reported in ppm, while coupling constants, *J*, are reported in Hertz. Multiplicities in the spectra are represented by d (doublet), t (triplet), m (multiplet), and b (broad). High-resolution mass spectra (HRMS) were recorded using a Waters Synapt G2; spectra are reported as m/z (relative intensity). 1 μL of saturated LiCl in acetonitrile was added to 50 μL of sample, masses are reported for either [M+] or [M+H$^+$] ion. Millipore water was obtained from a Milli-Q Advantage A-10 water purification system (MilliPore, USA). Microscopy images were captured using a Zeiss Axio Imager A2. Nanoparticle Tracking Analysis was performed on a Malvern NanoSight LM10.

Synthesis of reduced dye

2.5 mg (2.1 μmol) of 1,1′-dioctadecyl-3,3,3′3′-tetramethylindocarbocyanine perchlorate ($DiIC_{18}$(3), Molecular Probes) was dissolved in 1 mL 200 proof ethanol. 0.24 mg (6.3 μmol) of sodium borohydride (Acros Organics) in 100 μL in ethanol was added dropwise to the DiI solution with continuous stirring, followed by another 5–10 min stirring at RT to make a colorless solution. The ethanol was removed by rotary evaporator, followed by addition of 3 mL of chloroform. The chloroform was washed twice with 1 mL Millipore water and once with 1 mL brine, followed by drying over anhydrous magnesium sulfate, filtering through silica, and concentration by rotary evaporator. For storage, 1 mL of NEOBEE oil (Spectrum Chemical Mfg. Corp.) or soybean oil (MP Biomedicals, LLC) was then added to the flask and mixed in the rotary evaporator without vacuum for 10 min. The solution of reduced DiI in oil was stored in a glass vial wrapped with aluminum foil at 2–8 °C. ^{1}H NMR (400 MHz, $CDCl_3$): δ 7.17-7.07 (m, 4H, Ar-H), 7.03-7.01 (m, 2H, Ar-H), 6.83-6.75 (m, 2H, Ar-H),

6.68 (t, 1H, -CH=CH-CH=, *J* = 7.3 Hz), 6.55 (d, 1H, -CH=CH-CH=, *J* = 7.8 Hz) 6.47 (d, 1H, -CH=CH-CH=, *J* = 7.7 Hz), 5.41-5.32 (m, 2H, -CH=CH-CH=), 3.80-3.55 (m, 2H, N-CH_2-CH_2), 3.22-2.99 (m, 2H, N-CH_2-CH_2), 1.95-0.85 (82H, aliphatic region); ^{13}C NMR (100 MHz, $CDCl_3$): δ 154.34, 150.34, 145.29, 139.09, 138.59, 130.27, 127.58, 127.27, 121.68, 121.57, 121.40, 118.54, 116.98, 106.73, 105.48, 94.81, 78.42, 45.69, 45.03, 44.08, 42.26, 31.94, 29.71, 29.68, 29.63, 29.56, 29.48, 29.37, 28.33, 28.07, 27.40, 27.23, 26.31, 25.96, 25.89, 24.14, 22.70, 14.13. HRMS (ESI+) for $C_{59}H_{98}N_2$ [M+H$^+$]: calculated: 835.7808, experimental: 835.7792.

Activation studies of reduced dye

The following quinones were used for re-oxidation studies: p-fluoranil (Alfa Aesar), p-chloranil (Merck KGaA), 2,3-dichloro-5,6-dicyano-1,4-benzoquinone (DDQ, Acros Organics), 1,4-dihydroxyanthraquinone, (DHAQ, Acros Organics), 9,10-phenanthrenequinone (Chem-Impex Int'l Inc.), and 3,3′,5,5′-tetra-*tert*-butyldiphenoquinone (DPQ, TCI Co., Ltd.). For each study, a 2.14 mM solution of each of these reagents was made in NEOBEE oil to match the ~2.14 mM solution of HDiI in NEOBEE oil. Equal volumes of reduced DiI and the respective oxidizing agent were mixed for 5 min. Next, each solution was diluted 2000X in NEOBEE oil, and fluorescence measurements were recorded (λ_{exc} = 532 nm). Analogous experiments were also performed in soybean oil for HDiI and p-fluoranil. The fluorescence spectra of 1.07 mM solution of commercial DiI and HDiI alone were taken as a positive and negative control, respectively. Since a 1:4 molar ratio of reduced DiI:p-fluoranil proved optimal, NMR spectra for the reactivated DiI was recorded using this ratio. ^{1}H-NMR (400MHz, $CDCl_3$): δ 8.42 (b, 1H, -CH=CH-CH=), 7.39 (b, 2H, Ar-H), 7.27 (b, 2H, -CH=CH-CH=), 7.14 (b, 1H, Ar-H), 6.85 (b, 1H, Ar-H), 4.18 (b, 4H, N-CH_2-CH_2-), 1.88-0.85 (82H, aliphatic region); ^{13}C NMR (100 MHz, $CDCl_3$): δ 173.98, 142.14, 140.63, 128.87, 125.42, 122.13, 111.07, 103.36, 53.43, 49.16, 44.54, 31.93, 29.71, 29.66, 29.62, 29.46, 29.43, 29.37, 28.06, 27.53, 26.79, 22.69, 14.12. HRMS (ESI+) for $C_{59}H_{97}N_2$ [M+]: calculated: 833.7652, experimental: 833.7659.

Synthesis of anti-VEGF aptamer-maleimide conjugate

Prior to all experiments, Tris-buffered saline (TBS) was prepared to a final concentration of 10 nM Tris base (Fisher Scientific) and 100 mM NaCl (Fisher Scientific), adjusted to a pH of 7.4 with dilute HCl. A di-thiol modified version of an anti-VEGF aptamer (5′-/5ThioMC6-D/TTTTCCCGTCTTCCAGACAAGAGTGCAGGG-3′) was purchased from Integrated DNA Technologies. Modifying a literature procedure,[36] 100 μL of a 100 μM aptamer stock solution was mixed with 100 μL of 10mM aqueous solution (pH adjusted to 7.4) of Tris(2-carboxyethyl) phosphine hydrochloride (TCEP, Strem Chemicals Inc.), and reacted at 350rpm for 45 mins. Purification was carried out through a centrifugal filter (MWCO 3000 Da) at 4000 rcf for 20 mins, followed by washing twice with milipore water. 100 μL of the re-suspended final product containing the activated aptamer was mixed with 250 μL of a 2mg/mL DSPE-PEG2000-Maleimide (Avanti Polar Lipids, Inc.) solution in 1x PBS (Fisher Scientific), and reacted at 75°C for 1 hr. The product solution was then centrifuged under the same conditions mentioned previously, followed by washing in water, and then in TBS. The aptamer-maleimide product was re-suspended in TBS to form a final aptamer concentration of 100 μM.

Formulation of nanodroplets

For droplet formulation, a stock solution of DPPC (Avanti Polar Lipids, Inc.) was prepared as described previously.[2] DSPE-PEG2000 and DPSE-PEG2000-Biotin (both from Avanti Polar Lipids, Inc.) were individually dissolved in TBS and added to the stock DPPC solution to make a final concentration of 1.3 mM DPPC/40 μM DSPE-PEG2000/15 μM DSPE-PEG2000-Biotin. To make anti-VEGF aptamer coated nanodroplets, DSPE-PEG2000-Biotin was replaced by the aptamer-maleimide conjugate to a final concentration of 150 nM. This lipid-PEG-biotin (or lipid-PEG-aptamer) mixture was then stirred at 75°C for 30–40 min and allowed to cool to RT. Two NEOBEE oil solutions were prepared: one with 2.14 mM HDiI (**A**), and one with 8.56 mM p-fluoranil (**B**). 40 μL of either solution **A** or solution **B** was added per mL of the lipid-PEG-biotin (or lipid-PEG-aptamer) stock to make a 4 v/v% mixture, and probe-sonicated (Branson SLPe, 40 kHz) for two 1min cycles – 1s on, 9s off – at 70% amplitude. The emulsion was then centrifuged at 1500 *g* for 1 min, followed by drawing ~0.5 mL of the supernatant, making sure to avoid the pellet at the bottom and the flotsam on top; the supernatant was then centrifuged using a 0.45 μm centrifugal filter (VWR International) at 12,000 *g* for 4.5 min, followed by washing with TBS under the same conditions. The droplet pellet in the filter was resuspended in 150 μL TBS per mL emulsion centrifuged. Plain NEOBEE oil droplets (without either dye or p-fluoranil) were also prepared in the same way for characterizing droplet size distribution. Droplet size distribution and concentration was measured by NTA.

Aggregation of nanodroplets

Stock analyte solutions of streptavidin (Pierce) of varying concentrations were prepared in TBS (or HyClone-characterized Fetal Bovine Serum (FBS) or Bovine Plasma (Sodium Citrate) as required; FBS and Bovine Plasma were purchased from ThermoFisher Scientific and Pel-Freez Biologicals respectively). Stock solutions of Human VEGF-165 (Shenandoah Biotechnology Inc.) were also prepared in TBS. Next, 10 μL (or approximately $7.5x10^9$ droplets, as determined by NTA) each of HDiI and p-fluoranil droplets in TBS were mixed together. Additional 30 μL TBS was added, followed by 50 μL of an appropriate analyte stock solution to attain the analyte concentrations mentioned in the text and a total volume to 100 μL. (Biotinylated droplets were incubated with streptavidin, while aptamer-coated droplets were incubated with VEGF dimer) The mixture was shaken in a thermomixer (Eppendorf) at 37°C for 30 min. The samples were then imaged in epifluorescence mode in a red channel (Zeiss). 10 μL of each sample was taken and diluted to 1 mL in TBS for NTA characterization. For time-dependent studies of biotinylated droplet sample in the absence of streptavidin (Control), 10 μL of the same sample was characterized using the NTA setup after 0, 15, 30, 60, and 120 min after mixing and incubation.

Nanoparticle Tracking Analysis and fluorescence studies

Size distribution and concentration of NEOBEE oil droplets were determined using Nanoparticle Tracking Analysis. To determine fluorescent intensity of aggregated versus non-aggregated droplets, a push-pull fluorescence filter in the NanoSight setup was used, which allowed for visualization of fluorescent droplets/aggregates only, eliminating contribution to the response from the rest. Three 60 s videos were recorded for each sample:

in order to compare samples, criteria such as camera exposure level (maximum, at 16) and threshold detection level (18) were kept same for all experiments. The intensity vs. size data was analyzed by the NTA 3.0 software (Malvern). P-values were obtained using a one-tailed Student's t-test against the null hypothesis that the means were equal. Calculated values are given in Figure S6.

Supplementary Material

Refer to Web version on PubMed Central for supplementary material.

Acknowledgments

Funding Sources

NIH grants DP2EB020401, R21EB018034, and R00CA153935

This work was supported by NIH grants DP2EB020401, R21EB018034, and R00CA153935. The authors thank Dr. Omer Yehekzeli and Prof. Jennifer Cha for helpful discussions and Mr. Diego Chimendes for help with reagent synthesis. The authors would also like to thank the Central Analytical Lab at CU Boulder for their help with mass spectroscopy, which was supported by NIH grant S10RR026641.

ABBREVIATIONS

DiI	1,1′-dioctadecyl-3,3,3′3′-tetramethylindocarbocyanine perchlorate
HDiI	DiI reduced with $NaBH_4$
p-Fluoranil	tetrafluoro-1,4-benzoquinone
p-Chloranil	tetrachloro-1,4-benzoquinone
DDQ	2,3-Dichloro-5,6-dicyano-1,4-benzoquinone
DHAQ	1,4-Dihydroxyanthraquinone
DPPC	1,2-dipalmitoyl-sn-glycero-3-phosphocholine
DPQ	3,3′,5,5′-tetra-tertbutyldiphenoquinone
DSPE-PEG2000	1,2-distearoyl-sn-glycero-3-phosphoethanolamine-N-[amino(polyethylene glycol)-2000]
DSPE-PEG2000-Biotin	1,2-distearoyl-sn-glycero-3-phosphoethanolamine-N-[biotinyl(polyethylene glycol)-2000]

References

1. Weissleder R, Tung CH, Mahmood U, Bogdanov A. In Vivo Imaging of Tumors with Protease-Activated Near-Infrared Fluorescent Probes. Nat Biotechnol. 1999; 17:375–378. [PubMed: 10207887]
2. Jiang T, Olson ES, Nguyen QT, Roy M, Jennings PA, Tsien RY. Tumor Imaging by Means of Proteolytic Activation of Cell-Penetrating Peptides. Proc Natl Acad Sci U S A. 2004; 101:17867–17872. [PubMed: 15601762]

3. Santangelo PJ, Nix B, Tsourkas A, Bao G. Dual FRET Molecular Beacons for mRNA Detection in Living Cells. Nucleic Acids Res. 2004; 32:e57. [PubMed: 15084672]
4. Li JWJ, Chu YZ, Lee BYH, Xie XLS. Enzymatic Signal Amplification of Molecular Beacons for Sensitive DNA Detection. Nucleic Acids Res. 2008; 36
5. Tyagi S, Kramer FR. Molecular Beacons: Probes that Fluoresce upon Hybridization. Nat Biotechnol. 1996; 14:303–308. [PubMed: 9630890]
6. Elghanian R, Storhoff JJ, Mucic RC, Letsinger RL, Mirkin CA. Selective Colorimetric Detection of Polynucleotides Based on the Distance-Dependent Optical Properties of Gold Nanoparticles. Science. 1997; 277:1078–1081. [PubMed: 9262471]
7. Min C, Shao HL, Liong M, Yoon TJ, Weissleder R, Lee H. Mechanism of Magnetic Relaxation Switching Sensing. ACS Nano. 2012; 6:6821–6828. [PubMed: 22762250]
8. Nam JM, Thaxton CS, Mirkin CA. Nanoparticle-based Bio-bar Codes for the Ultrasensitive Detection of Proteins. Science. 2003; 301:1884–1886. [PubMed: 14512622]
9. Lee JH, Domaille DW, Cha JN. Amplified Protein Detection and Identification through DNA-Conjugated M13 Bacteriophage. ACS Nano. 2012; 6:5621–5626. [PubMed: 22587008]
10. Hamaguchi N, Ellington A, Stanton M. Aptamer Beacons for the Direct Detection of Proteins. Anal Biochem. 2001; 294:126–131. [PubMed: 11444807]
11. Wang K, Tang Z, Yang CJ, Kim Y, Fang X, Li W, Wu Y, Medley CD, Cao Z, Li J, Colon P, Lin H, Tan W. Molecular Engineering of DNA: Molecular Beacons. Angew Chem Int Ed. 2009; 48:856–870.
12. Chen AK, Behlke MA, Tsourkas A. Avoiding False-positive Signals with Nuclease-Vulnerable Molecular Beacons in Single Living Cells. Nucleic Acids Research. 2007; 35:e105. [PubMed: 17702767]
13. Mohan P, Noonan PS, Nakatsuka MA, Goodwin AP. On-Demand Droplet Fusion: A Strategy for Stimulus-Responsive Biosensing in Solution. Langmuir. 2014; 30:12321–12327. [PubMed: 25263344]
14. Noonan PS, Mohan P, Goodwin AP, Schwartz DK. DNA Hybridization-Mediated Liposome Fusion at the Aqueous Liquid Crystal Interface. Adv Funct Mater. 2014; 24:3206–3212. [PubMed: 25506314]
15. Miller EW, Tulyathan O, Isacoff EY, Chang CJ. Molecular Imaging of Hydrogen Peroxide Produced for Cell Signaling. Nat Chem Biol. 2007; 3:349–349.
16. Miller EW, Albers AE, Pralle A, Isacoff EY, Chang CJ. Boronate-based Fluorescent Probes for Imaging Cellular Hydrogen Peroxide. J Am Chem Soc. 2005; 127:16652–16659. [PubMed: 16305254]
17. Terai T, Nagano T. Fluorescent Probes for Bioimaging Applications. Curr Opin Chem Biol. 2008; 12:515–521. [PubMed: 18771748]
18. Umezawa N, Tanaka K, Urano Y, Kikuchi K, Higuchi T, Nagano T. Novel Fluorescent Probes for Singlet Oxygen. Angew Chem Int Ed. 1999; 38:2899–2901.
19. Setsukinai K, Urano Y, Kakinuma K, Majima HJ, Nagano T. Development of Novel Fluorescence Probes that Can Reliably Detect Reactive Oxygen Species and Distinguish Specific Species. J Biol Chem. 2003; 278:3170–3175. [PubMed: 12419811]
20. Fitch KR, Goodwin AP. Mechanochemical Reaction Cascade for Sensitive Detection of Covalent Bond Breakage in Hydrogels. Chem Mater. 2014; 26:6771–6776.
21. Kundu K, Knight SF, Willett N, Lee S, Taylor WR, Murthy N. Hydrocyanines: a Class of Fluorescent Sensors that Can Image Reactive Oxygen Species in Cell Culture, Tissue, and in Vivo. Angew Chem Int Ed. 2009; 48:299–303.
22. Kundu K, Knight SF, Lee S, Taylor WR, Murthy N. A Significant Improvement of the Efficacy of Radical Oxidant Probes by the Kinetic Isotope Effect. Angew Chem Int Ed. 2010; 49:6134–6138.
23. Oushiki D, Kojima H, Terai T, Arita M, Hanaoka K, Urano Y, Nagano T. Development and Application of a Near-Infrared Fluorescence Probe for Oxidative Stress Based on Differential Reactivity of Linked Cyanine Dyes. J Am Chem Soc. 2010; 132:2795–2801. [PubMed: 20136129]
24. Zhu XQ, Wang CH, Liang H. Scales of Oxidation Potentials, pK_a, and BDE of Various Hydroquinones and Catechols in DMSO. J Org Chem. 2010; 75:7240–7257. [PubMed: 20873851]

25. Filipe V, Hawe A, Jiskoot W. Critical Evaluation of Nanoparticle Tracking Analysis (NTA) by NanoSight for the Measurement of Nanoparticles and Protein Aggregates. Pharm Res. 2010; 27:796–810. [PubMed: 20204471]
26. Chattaraj R, Mohan P, Besmer JD, Goodwin AP. Selective Vaporization of Superheated Nanodroplets for Rapid, Sensitive Acoustic Biosensing. Adv Healthcare Mater. 2015; 4:1790–1795.
27. Mason HS. Reactions between Quinones and Proteins. Nature. 1955; 175:771–772.
28. Li WW, Heinze J, Haehnel W. Site-Specific Binding of Quinones to Proteins through Thiol Addition and Addition—Elimination Reactions. J Am Chem Soc. 2005; 127:6140–6141. [PubMed: 15853297]
29. Freeman R, Girsh J, Jou AF, Ho JA, Hug T, Dernedde J, Willner I. Optical Aptasensors for the Analysis of the Vascular Endothelial Growth Factor (VEGF). Anal Chem. 2012; 84:6192–6198. [PubMed: 22746189]
30. Zhao Z, Al-Ameen MA, Duan K, Ghosh G, Lo JF. On-chip Porous Microgel Generation for Microfluidic Enhanced VEGF Detection. Biosens Bioelectron. 2015; 74:305–312. [PubMed: 26148675]
31. Lee JH, Wark AW, Corn RM. Microarray Methods for Protein Biomarker Detection. Analyst. 2008; 133:975–983. [PubMed: 18645635]
32. Xu X, Wang B, Ye C, Yao C, Lin Y, Huang X, Zhang Y, Wang S. Overexpression of Macrophage Migration Inhibitory Factor Induces Angiogenesis in Human Breast Cancer. Cancer Lett. 2008; 261:147–157. [PubMed: 18171602]
33. Muller YA, Li B, Christinger HW, Wells JA, Cunningham BC, de Vos AM. Vascular Endothelial Growth Factor: Crystal Structure and Functional Mapping of the Kinase Domain Receptor Binding Site. Proc Natl Acad Sci U S A. 1997; 9(4):7192–7197. [PubMed: 9207067]
34. Potty AS, Kourentzi K, Fang H, Jackson GW, Zhang X, Legge GB, Willson RC. Biophysical Characterization of DNA Aptamer Interactions with Vascular Endothelial Growth Factor. Biopolymers. 2009; 91:145–156. [PubMed: 19025993]
35. Zhang X, Yadavalli VK. Surface Immobilization of DNA Aptamers for Biosensing and Protein Interaction Analysis. Biosens Bioelectron. 2011; 26:3142–3147. [PubMed: 21227676]
36. Wang CH, Kang ST, Lee YH, Luo YL, Huang YF, Yeh CK. Aptamer-conjugated and Drug-loaded Acoustic Droplets for Ultrasound Theranosis. Biomaterials. 2012; 33:1939–1947. [PubMed: 22142768]

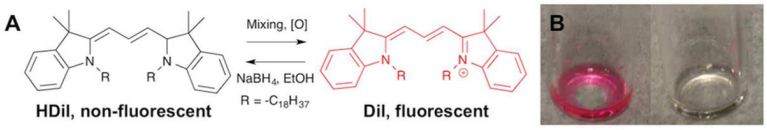

Figure 1.

A: Scheme of reduction of DiI by NaBH4 and reactivation by oxidants. B: HDiI (right) and HDiI reactivated with 1 molar equivalent of p-fluoranil (left) in NEOBEE oil.

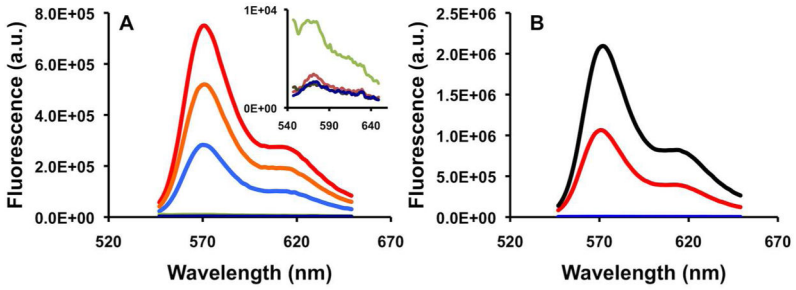

Figure 2.

Fluorescence emission spectra (λ_{exc} = 532 nm) of mixtures of HDiI and various oxidants. **A**: Spectra of 1:1 mixtures of HDiI and p-fluoranil (red), p-chloranil (orange), DDQ (light blue), DHAQ (light green), 9,10-phenanthrenequinone (light red), DPQ (dark green), and HDiI only (dark blue); the latter four are shown magnified in the *inset*. B: Commercial DiI only (black), 1:4 HDiI:p-fluoranil (dark red), and HDiI only (blue).

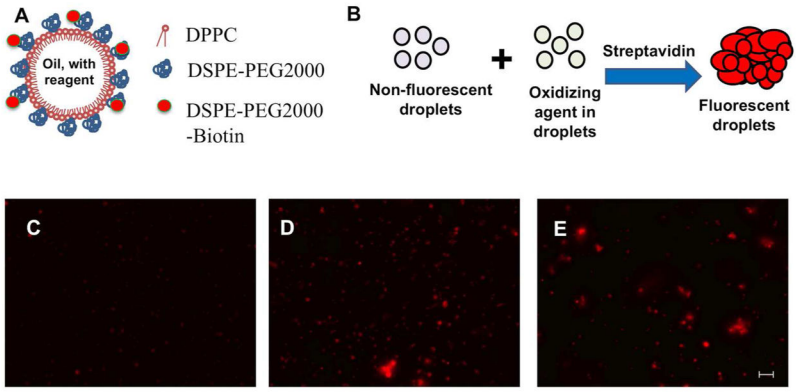

Figure 3.

A: Schematic of droplet structure. B: Schematic of nanodroplet composition and aggregation scheme. C–E: False-colored fluorescence microscopy images of mixed HDiI droplets and p-fluoranil droplets with 0 (C), 25 nM (D), and 1 μM (E) streptavidin. Scale bar: 5 μm

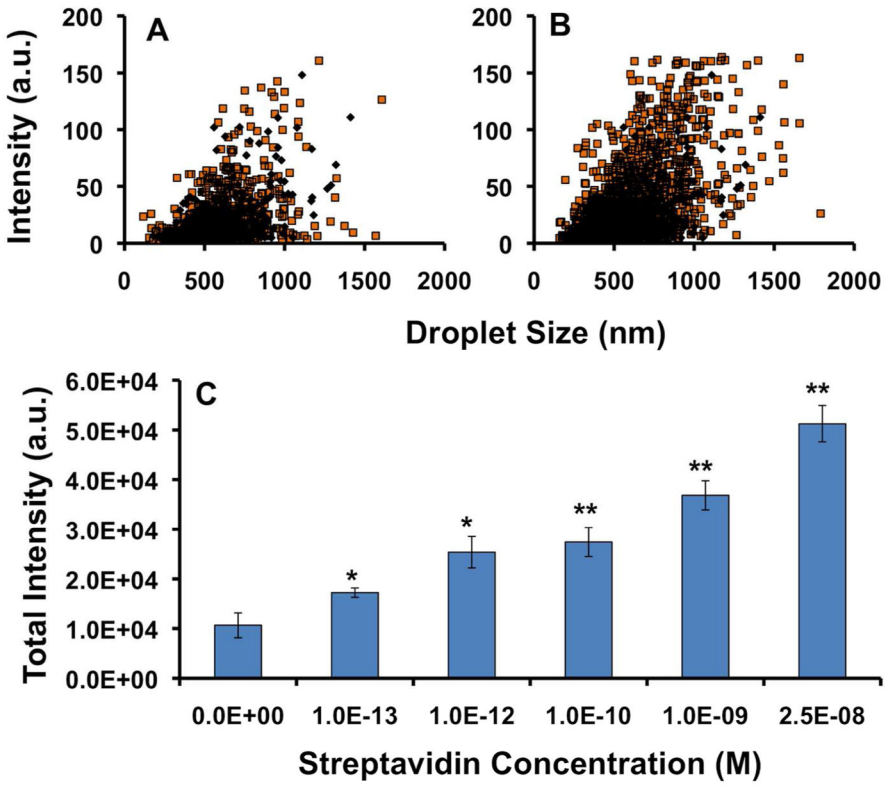

Figure 4.

A–B: Representative NTA fluorescence scatter plots of biotinylated HDiI droplets and p-fluoranil droplets mixed without (black diamonds) or with (orange squares) a respective concentration of streptavidin (**A**: 100 fM; **B**: 25 nM); **C**: Dose response of mixed HDiI droplets and p-fluoranil droplets as a function of streptavidin concentration. Integrated intensity is the summation of intensity of each detected droplet aggregate. Error bars represent standard deviation of at least three trials. *p<0.05, **p<0.005 as compared to sample without streptavidin.

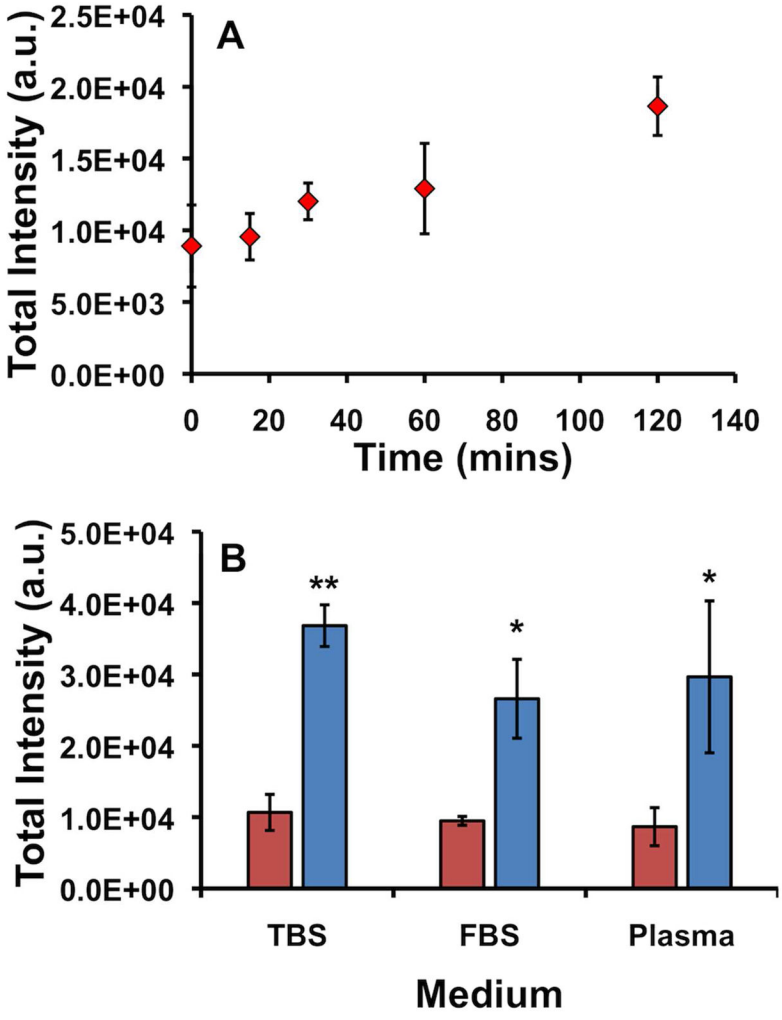

Figure 5.

A: Time-dependent response of mixed biotinylated HDiI droplets and p-fluoranil droplets in the absence of streptavidin. **B**: Response of the mixed droplets without (*red*) or with (*blue*) 1 nM streptavidin in TBS, 50% FBS, or 50% Bovine Plasma. *p<0.05, **p<0.005 as compared to sample without streptavidin.

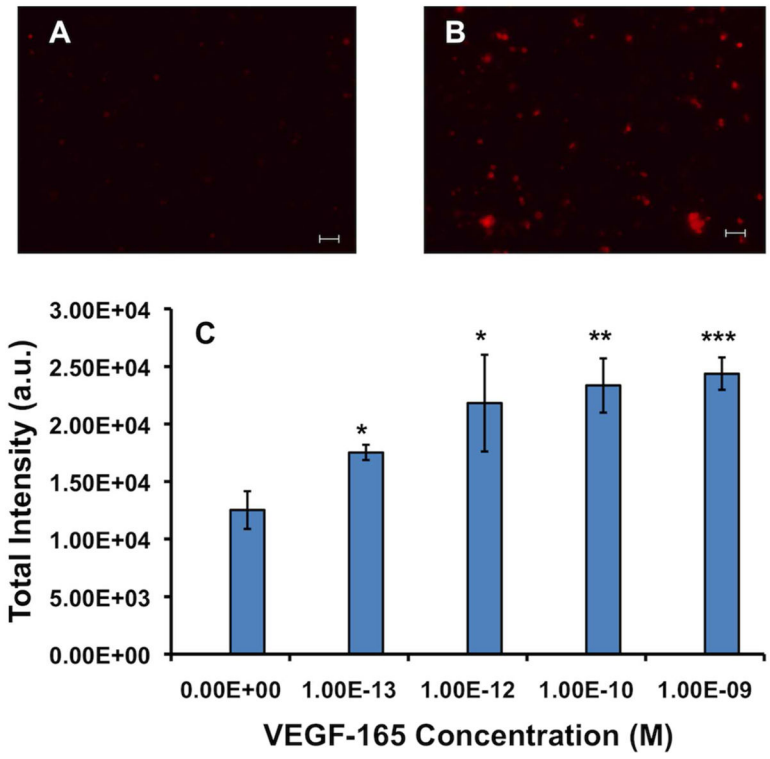

Figure 6.

A–B: False-colored fluorescence microscopy images of anti-VEGF aptamer coated mixed HDiI droplets and p-fluoranil droplets incubated with 0 (A) and 100 nM (B) VEGF-165. Scale bar: 5 μm; **C**: Dose response of the mixed droplets as a function of VEGF-165 concentration. **P*<0.05, ***P*<0.005, ****P*<0.0005, Student's *t*-test compared to sample without VEGF.